Interplanetary coronal mass ejections in the near-Earth solar wind during 1996–2002

H. V. Cane[1] and I. G. Richardson[2]

Laboratory for High Energy Astrophysics, NASA Goddard Space Flight Center, Greenbelt, Maryland, USA

[1]   We summarize the occurrence of interplanetary coronal mass ejections (ICMEs) in the near-Earth solar wind during 1996–2002, corresponding to the increasing and maximum phases of solar cycle 23. In particular, we give a detailed list of such events. This list, based on in situ observations, is not confined to subsets of ICMEs, such as "magnetic clouds" or those preceded by "halo" coronal mass injections (CMEs) observed by the Solar and Heliospheric Observatory/Large Angle and Spectrometric Coronagraph, and provides an overview of 214 ICMEs in the near-Earth solar wind during this period. The ICME rate increases by about an order of magnitude from solar minimum to solar maximum (when the rate is ∼3 ICMEs per solar rotation period). The rate also shows a temporary reduction during 1999 and another brief, deeper reduction in late 2000 to early 2001, which only approximately track variations in the solar 10-cm flux. In addition, there are occasional periods of several rotations duration when the ICME rate is enhanced in association with high solar activity levels. We find an indication of a periodic variation in the ICME rate, with a prominent period of ∼165 days similar to that previously reported in various solar phenomena. It is found that the fraction of ICMEs that are magnetic clouds has a solar cycle variation, the fraction being larger near solar minimum. For the subset of events that we could associate with a CME at the Sun the transit speeds from the Sun to the Earth were highest after solar maximum.   *INDEX TERMS:* 2111 Interplanetary Physics: Ejecta, driver gases, and magnetic clouds; 7513 Solar Physics, Astrophysics, and Astronomy: Coronal mass ejections; 2139 Interplanetary Physics: Interplanetary shocks; 2162 Interplanetary Physics: Solar cycle variations (7536); *KEYWORDS:* interplanetary coronal mass ejections, coronal mass ejections, solar wind, magnetic clouds, solar cycle variation

1. Introduction

[2] Material in the solar wind now believed to be the interplanetary counterpart of coronal mass ejections (CMEs) at the Sun has been identified since the early years of solar wind observations. By the early 1980s, most of the characteristic signatures of such materials, which we here term "interplanetary coronal mass ejections" (ICMEs), had been identified, as reviewed by *Gosling* [1990] and *Neugebauer and Goldstein* [1997]. (Older terms used for ICMEs include "driver gas" and "ejecta.") Combined in situ measurements by the Helios spacecraft off the limbs of the Sun and observations by the Solwind coronagraph demonstrated the clear association between CMEs at the Sun and shocks and ICMEs subsequently detected in the interplanetary medium [*Sheeley et al.*, 1985]. Solar wind plasma signatures of ICMEs include abnormally low proton temperatures [e.g., *Gosling et al.*, 1973; *Richardson and Cane*, 1995], low electron temperatures [e.g., *Montgomery et al.*, 1974], and bidirectional suprathermal electron strahls [e.g., *Zwickl et al.*, 1983; *Gosling et al.*, 1987].

[3] Plasma compositional anomalies have also been identified in ICMEs, including enhanced plasma helium abundances relative to protons [e.g., *Hirshberg et al.*, 1972; *Borrini et al.*, 1982] and occasional enhancements in minor ions (in particular iron) [*Bame et al.*, 1979; *Mitchell et al.*, 1983; *Ipavich et al.*, 1986]. Enhanced Fe charge states have also been reported [*Bame et al.*, 1979; *Fenimore*, 1980; *Ipavich et al.*, 1986; *Lepri et al.*, 2001]. Such enrichments suggest that the plasma inside ICMEs originates in the low corona. Energetic particle signatures include bidirectional energetic protons [e.g., *Palmer et al.*, 1978; *Marsden et al.*, 1987; *Richardson and Reames*, 1993] and cosmic rays [*Richardson et al.*, 2000], energetic particle intensity depressions (Forbush decreases) [e.g., *Morrison*, 1956; *Barnden*, 1972; *Cane et al.*, 1994], and unusual solar energetic particle (SEP) flow directions [*Richardson et al.*, 1991; *Richardson and Cane*, 1996]. The bidirectional particle flows (suprathermal electron

---

[1]Also at School of Mathematics and Physics, University of Tasmania, Hobart, Australia.

[2]Also at Department of Astronomy, University of Maryland, College Park, Maryland, USA.

strahls and energetic particles), unusual solar particle event flows, and energetic particle intensity depressions are consistent with the presence within many ICMEs of regions of looped magnetic field lines rooted at the Sun at both ends.

[4] A subset of ICMEs have simple flux rope-like magnetic fields, characterized by enhanced magnetic fields that rotate slowly through a large angle. Such "magnetic clouds" [*Burlaga et al.*, 1981; *Klein and Burlaga*, 1982] have received considerable attention because the magnetic field configuration is amenable to simple modeling [e.g., *Lepping et al.*, 1990; *Osherovich and Burlaga*, 1997, and references therein] and may be consistent with helical structures occasionally present in coronagraph observations of CMEs [e.g., *Dere et al.*, 1999]. Magnetic clouds are also responsible for some major geomagnetic storms [e.g., *Webb et al.*, 2000].

[5] As has been noted by many authors, however [e.g., *Zwickl et al.*, 1983; *Crooker et al.*, 1990; *Richardson and Cane*, 1993, 1995; *Neugebauer and Goldstein*, 1997], individual signatures may not be detected in all ICMEs, either because they are not present or as a result of instrumental limitations or data gaps. Some signatures have been reported relatively infrequently. For example, *Zwickl et al.* [1982] found only three distinct He$^+$ events in 8 years of IMP 7 and 8 and ISEE 1 and 3 observations. Other signatures, such as proton temperature depressions, are generally present [e.g., *Richardson and Cane*, 1995]. Furthermore, even if several signatures are present in an ICME, they do not necessarily coincide exactly. Hence, to make a comprehensive identification of ICMEs, observations of as many signatures as possible should be considered. Those signatures that are most frequently present are of particular value.

[6] Our own interest in ICMEs lies in several areas: One interest is the effects of ICMEs on energetic particles. Our studies suggest that these effects generally do not depend strongly on the nature of the in situ signatures. This is not too surprising since presumably it is the large-scale topology of the ICME field lines (i.e., whether they are predominantly closed) that is important in modulating the particle intensity, not the magnetic fields that are observed along the particular trajectory of a spacecraft through the ICME. Another of our interests is the contribution of ICMEs to geomagnetic activity, both storms and long-term averages [e.g., *Cane et al.*, 2000; *Richardson et al.*, 2001a, 2002].

[7] Hence, as a contribution to such studies, we have maintained a list of ICMEs at Earth which extends back to the earliest in situ observations. This is relatively comprehensive because our interest is not limited to a subset of events with particular signatures. This list has evolved and expanded with our various studies related to ICMEs in the inner heliosphere, many of which are referenced in this paper. These studies also illustrate many examples of ICMEs which help to demonstrate the wide event-to-event diversity in the various ICME signatures and their interrelationships.

[8] In this paper, we concentrate on events in 1996–2002, during the increasing phase and maximum of solar cycle 23. During the current solar cycle, coronal mass ejections at the Sun have been regularly monitored by the Solar and Heliospheric Observatory (SOHO) spacecraft

since its launch in December 1995. The Large Angle and Spectrometric Coronagraph (LASCO) [*Brueckner et al.*, 1995] is more sensitive to structures moving out of the plane of the sky than previous coronagraphs and has observed a significant number of CMEs which surround the Sun (angular extents of 360°) that may be directed approximately along the Sun-Earth line (similar events originating on the backside of the Sun and moving away from Earth are also seen). Various studies have linked apparently Earthward-directed CMEs with in situ observations of ICMEs at 1 AU, focusing, for example, on their geomagnetic effects or transit times [e.g., *Webb et al.*, 2000; *Cane et al.*, 1998a, 2000; *Gopalswamy et al.*, 2000, 2001; *Wang et al.*, 2002]. However, such studies have not attempted to provide a comprehensive survey of ICMEs in the vicinity of Earth starting from the in situ observations, which is the purpose of the present paper.

2. List

[9] The principle data sets we routinely use for the identification of potential ICMEs are solar wind plasma and magnetic field observations. A major reason is that such data are readily available since the beginning of the space era. Since it appears to be a common feature of most ICMEs [e.g., *Richardson and Cane*, 1993, 1995], one of our primary identifying signatures is the occurrence of abnormally low proton temperatures. To identify such plasma, we use the method of *Richardson and Cane* [1993, 1995], which compares, point by point, the observed proton temperature (T_p) with the "expected" temperature (T_{ex}) appropriate for "normally expanding" solar wind with the observed solar wind speed (V_{sw}). The expected temperature is essentially the typical temperature found in normal solar wind with speed V_{sw} and is inferred using the well-established correlation between the solar wind speed and T_p [e.g., *Burlaga and Ogilvie*, 1973; *Lopez*, 1987], which, however, may be slightly instrument-dependent (see the discussion in *Neugebauer et al.* [2003]). We find that many ICMEs are characterized by $T_p/T_{ex} < 0.5$ [e.g., *Richardson and Cane*, 1995].

[10] Having identified periods of interest based on T_p, we typically examine magnetic field observations during these periods, ideally at a time resolution of 5 min or less. Frequently, in ICMEs the field is directed far from the Parker spiral in azimuth or has large out-of-the-ecliptic components. A useful characteristic is a reduction in the level of field fluctuations which can be identified by eye in data with this time resolution. In some cases a clear magnetic cloud signature is present. In other ICMEs there is often evidence of an organized field rotation, but the signature does not conform to the strict cloud definition of *Burlaga et al.* [1981] and *Klein and Burlaga* [1982]. Alternatively, there may be no distinct rotation, two extremes being a magnetic field that is relatively constant in direction and one that includes many discontinuities in direction which may be related to internal structure. In summary, most often, a likely ICME interval can be inferred from reduced fluctuations and some degree of organization in the magnetic field and is bounded by distinct magnetic field discontinuities which may be accompanied by abrupt changes in plasma parameters. Typically, this interval cor-

responds reasonably well with the T_p depression, though in some ICMEs they may differ significantly. There are also occasional ICMEs (based on the presence of other ICME signatures) that do not have well-characterized field signatures. One other point to note is that although ICMEs can include strong magnetic fields, such fields are not characteristic of all ICMEs.

[11] We also consider additional complementary signatures that may be indicative of the presence of ICMEs. One is the occurrence of interplanetary shocks. Fast ICMEs may generate shocks ahead of them so that an ICME is often located a few hours following the passage of a shock. Note, however, that an ICME is not present following every shock because the flanks of a shock extend well beyond the associated ICME [e.g., *Borrini et al.*, 1982; *Cane*, 1988; *Richardson and Cane*, 1993]. If the ICME is not sufficiently fast to generate a shock, there is sometimes evidence of an upstream wave-like disturbance that has not steepened into a shock. In other cases, if the ICME is convected out with the ambient solar wind, there may be no clear upstream feature. In addition to examining the solar wind data for evidence of shocks and referring to available lists of shocks, we refer to reports of geomagnetic storm sudden commencements (SCs), which are generally (but not always) associated with shocks passing the Earth (although almost all stronger shocks are accompanied by SCs; an exception is when the geomagnetic field is already disturbed). Such reports are particularly helpful when no in situ solar wind observations are available, though this is not a concern during the period considered in this paper.

[12] We routinely compare the solar wind observations with simultaneous energetic ($\sim$1–220 MeV) particle observations from the Goddard Medium Energy (GME) experiment on IMP 8 [*McGuire et al.*, 1986] and with higher-energy (GeV) cosmic ray observations from neutron monitors. Solar energetic particle events can help to relate shocks and ICMEs with specific solar events occurring $\sim$2 days earlier via their intensity-time profiles. An abrupt SEP intensity decrease a few hours following a shock usually indicates entry into the ICME because the shock-accelerated ions have difficulty entering the closed field lines of the ICME. An abrupt decrease in the galactic cosmic ray intensity may also occur at this time. When combined with the preceding decrease that often occurs at shock passage, this produces the classic "two step" cosmic ray Forbush decrease [*Cane*, 2000, and references therein]. The IMP 8 GME anticoincidence guard is a useful cosmic ray monitor for this purpose provided that the background from solar particle events is not too high [e.g., *Cane et al.*, 1994, 1998a]. The rigidity response is also lower than that of neutron monitors, which means that a larger counting rate depression will be seen in response to an ICME since the depression size decreases with increasing rigidity. In general, arrival of an ICME at Earth produces some detectable decrease in the cosmic ray intensity measured by IMP 8, followed by a recovery after the ICME has passed by. With familiarity with the data, ICME-related depressions can frequently be identified even without first referring to the solar wind parameters. However, the particle signatures can also be more subtle and can merely add to the evidence of the presence of an ICME.

[13] Although energetic particle observations play a supporting role to plasma and magnetic field observations when such observations are continuously available (as in cycle 23), they are useful in assessing the presence of solar wind structures when solar wind data are intermittent or nonexistent, such as in the early space era and in cycle 22 [e.g., *Cane et al.*, 1996]. The IMP 8 GME also provides information on the presence of bidirectional energetic particle flows, which can be indicative of ICMEs provided that the particle intensity is sufficiently high and that the spacecraft is located in the solar wind [e.g., *Richardson et al.*, 2001b, and references therein].

[14] One of the most widely used signatures in ICME identification is the presence of bidirectional solar wind electron strahls (BDEs). Although many researchers regard this as the most reliable signature, and indeed some studies identify ICMEs largely on this signature, we do not use BDEs as the primary signature. One reason, more relevant for our longer-term studies, is that BDE observations are only available for relatively limited intervals since in situ solar wind observations began. Another reason is that BDEs are known to be absent in some regions of ICMEs, apparently where ICME magnetic field lines have reconnected with the ambient solar wind, removing the heat flux in one direction [*Gosling et al.*, 1995]. In some of our previous studies, we noted that, occasionally, BDEs are detected that do not appear to be associated with ICMEs or that may extend beyond ICME regions that are distinguished in other data [e.g., *Richardson and Cane*, 1993]. Observations from the ACE spacecraft [*Gosling et al.*, 2001] also suggest that electron distributions may be complicated by counterstreaming set up by mirroring at magnetic field enhancements. It would have been interesting to compare our ICME identifications with intervals of BDEs, but unfortunately, there is no list of BDEs in the public domain for most of the period of our study at the time of writing.

[15] In our ICME identification we do not currently routinely incorporate plasma composition data. Again, one reason is that such data have been less consistently available in the past than the basic solar wind parameters. In addition, anomalous solar wind charge states and compositions are a subject of ongoing research, and their association with ICMEs remains to be fully explored. Thus our independent ICME list can provide a useful cross-reference for such studies [e.g., *Lepri et al.*, 2001].

[16] The estimated event boundaries given in this paper are therefore inferred from a consensus of the available signatures with an emphasis on those in the solar wind plasma and magnetic field. Typically, these boundaries can be associated with distinct plasma/magnetic field discontinuities. In other cases the boundaries are less pronounced but can be identified to within a relatively short period.

[17] The probable ICMEs that we have identified are listed in Table 1. The first column indicates the estimated time of the related disturbance in the upstream solar wind, if present. This may be a distinct shock or a small increase in the solar wind parameters which suggests a "bow wave." The SC time is given if one occurred. In this case, the SC strength (fifth column) has been calculated by the method of *Cane* [1985] in which the SC strengths reported by stations at geomagnetic latitudes of $5°$–$50°$ are averaged. *Cane*

Table 1. Near-Earth Interplanetary Coronal Mass Ejections (ICMEs), 1996–2002[a]

Disturbance Time,[b] UT	ICME Start, UT	ICME End, UT	Quality[c]	SC,[d] γ	V_{ICME}, km s^{-1}	V_{max}, km s^{-1}	B, nT	MC[e]	Dst, nT	V_T, km s^{-1}	LASCO CME[f]
					1996						
27 May 1500	27 May 1500	29 May 0000	2		370	400	9	2	−33		
1 July 1320	1 July 1800	2 July 1100	2	0	360	370	10	2	−20		
7 Aug 1300	7 Aug 1300	8 Aug 1000	2		350	380	7	2	−23		
23 Dec 1600	23 Dec 1700	25 Dec 1000	2		360	420	10	2	−18	480	19 Dec 1630[g]
					1997						
10 Jan 0104	10 Jan 0400	11 Jan 0200	1	9	450	460	14	2	−78	507	6 Jan 1510[g]
9 Feb 1321	10 Feb 0200	10 Feb 1900	1	22	450	600	8	2	−68	681	7 Feb 0030[g]
16 Feb 1600	16 Feb 2300	17 Feb 1800	1		350	350	9	1	−54		
10 April 1745	11 April 0600	11 April 2000	1	0	430	420	22	0	−82	552	7 April 1427[g]
21 April 0600	21 April 1000	23 April 0400	2		400	400	12	2	−107		
15 May 0159	15 May 0900	16 May 0000	1	33	450	430	23	2	−115	610	12 May 0630[g]
26 May 0957	26 May 1600	27 May 1000	2	2	350	350	10	1	−74	381	21 May 2100
8 June 1636	8 June 1800	10 June 0000	2	0	380	400	12	2	−84		
19 June 0032	19 June 0700	20 June 2300	2	0	360	390	8	2	−36		
15 July 0311	15 July 0800	16 July 1100	1	0	350	360	12	2	−45		
3 Aug 1042	3 Aug 1300	4 Aug 0300	1	0	400	480	16	2	−48	400	30 July 0445[g]
17 Aug 0200	17 Aug 0600	17 Aug 2000	1		390	410	7	0	−28		
3 Sep 0800	3 Sep 1300	3 Sep 2100	1		400	490	15	0	−98	390	30 Aug 0130[g]
17 Sep 0800	17 Sep 1600	18 Sep 0200	1		330	350	8	2	−45		
21 Sep 1651	21 Sep 2100	22 Sep 1600	1	0	450	470	20	2	−36	440	17 Sep 2028[g]
1 Oct 0059	1 Oct 1600	2 Oct 2300	2	23	450	470	10	2	−98	580	28 Sep 0108[g]
10 Oct 1612	10 Oct 2200	12 Oct 0000	1	15	400	450	12	2	−130	400	6 Oct 1528
26 Oct 1200	27 Oct 0000	28 Oct 0700	2		500	520	7	1	−60	470	23 Oct 1126[g]
6 Nov 2248	7 Nov 0400	9 Nov 1200	1	33	400	460	15	2	−11	640	4 Nov 0610[g]
22 Nov 0949	22 Nov 1500	23 Nov 1400	2	34	510	510	17	2	−108	600	19 Nov 1227[g]
Dec 10 0526	Dec 10 1800	Dec 12 0000	1	32	350	380	15	0	−60	460	6 Dec 1027
Dec 30 0209	Dec 30 1200	Dec 31 1100	3	11	390	360	12	1	−77	430	26 Dec 0231
					1998						
6 Jan 1416	7 Jan 0100	8 Jan 2200	2	29	400	410	16	2	−83	480	2 Jan 2328[g]
9 Jan 0700	9 Jan 0700	10 Jan 0800	2		450	500	6	0	−45		
20 Jan 0000	20 Jan 1700	21 Jan 0400	2		430	450	5	1	−42		
21 Jan 0400	21 Jan 0600	22 Jan 1300	3		380	400	12	0	−27	430	17 Jan 0409[g]
29 Jan 1800	29 Jan 1400	31 Jan 0100	2		350	400	7	0	−72	430	25 Jan 1526[g]
4 Feb 0000	4 Feb 0400	5 Feb 2300	1		320	390	11	2	−50		
17 Feb 0400	17 Feb 1000	17 Feb 2100	2		400	400	12	1	−102	602	14 Feb 0655
18 Feb 0750[h]	18 Feb 2300	20 Feb 0000	2		440	460	9	1	−66		
4 March 1156	4 March 1300	6 March 0900	1	0	350	380	12	2	−56	430	28 Feb 1248
6 March 0300	6 March 1500	7 March 1600	1		330	330	7	1	−25		
25 March 1000	25 March 1300	26 March 1000	1		400	400	10	0	−72		
11 April 2300	11 April 2300	13 April 1800	3		390	390	8	0	−56		
1 May 2156	2 May 0500	3 May 1700	2	29	520	650	10	2	−100	780	29 April 1658[g]
4 May 0215[h]	4 May 1000	8 May 0000	3		550	780	12	0	−216	1120	2 May 1406[g,i]
15 May 1451	15 May 2300	16 May 0800	2	0	400	340	15	0	−14		
29 May 1536	29 May 2200	30 May 1600	3	0	700	700	10	1	−58		
2 June 0800	2 June 1000	2 June 1800	2		390	400	11	2	−14		
13 June 1925	14 June 0400	15 June 0600	2	0	350	400	11	1	−68		
24 June 1000	24 June 1300	25 June 2100	2		450	540	13	2	−33		21 June 0535[j]
25 June 1636	26 June 0600	26 June 1900	1	0	460	490	10	0	−111		
5 July 0500	6 July 0600	9 July 0700	1		450	630	5	0	−37		DG
10 July 2300	11 July 0000	13 July 1500	2		400	400	10	0	−45		DG
30 July 2333	31 July 0600	31 July 1600	3	0	410	430	13	1	−51		DG
1 Aug 0400	1 Aug 0400	3 Aug 0300	3		410	450	7	1	−30		DG
5 Aug 1300	5 Aug 1300	6 Aug 1200	2		360	420	13	1	−166		DG
7 Aug 1800	7 Aug 2300	9 Aug 2300	2		450	500	7	0	−73		DG
10 Aug 0046	10 Aug 1100	11 Aug 0800	3	11	400	500	8	0	−37		DG
11 Aug 2300	12 Aug 0100	13 Aug 1400	3		380	420	7	1	−28		DG
19 Aug 1847	20 Aug 0600	21 Aug 2000	1	0	300	340	14	2	−86		DG
26 Aug 0651	26 Aug 2200	28 Aug 0000	2	53	650	860	14	0	−188	1260	DG (24 Aug 2200)
24 Sep 2345	25 Sep 0600	26 Sep 1600	1	45	620	770	20	2	−234	1150	DG (23 Sep 1100)
18 Oct 1952	19 Oct 0400	20 Oct 0700	2	22	400	410	18	2	−139	507	15 Oct 1004[g]
23 Oct 1230[h]	23 Oct 1900	25 Oct 1000	3		500	600	5	0	−60		
7 Nov 0815	7 Nov 2200	8 Nov 1200	2	13	450	530	15	1	−92	550	4 Nov 0418[g]
8 Nov 0451	8 Nov 1900	10 Nov 2000	2	0	450	640	12	2	−148	730	5 Nov 2044[g]
12 Nov 0143	13 Nov 0200	14 Nov 1200	2	0	390	400	17	0	−134	520	9 Nov 1818
30 Nov 0507	30 Nov 0900	1 Dec 0600	3	24	400	470	8	0	0		
28 Dec 1826	29 Dec 1800	31 Dec 0200	2	11	400	410	8	0	−53		DG

Table 1. (continued)

Disturbance Time,[b] UT	ICME Start, UT	ICME End, UT	Quality[c]	SC,[d] γ	V_{ICME}, km s^{-1}	V_{max}, km s^{-1}	B, nT	MC[e]	Dst, nT	V_T, km s^{-1}	LASCO CME[f]
					1999						
4 Jan 0000	4 Jan 0400	4 Jan 2200	3		350	360	8	0	−28		DG
13 Jan 1054	13 Jan 1500	13 Jan 2200	2	18	420	420	20	0	−113		DG
22 Jan 1950[h]	23 Jan 0900	24 Jan 0200	3		530	670	12	0	−49		DG
13 Feb 1900	13 Feb 1900	14 Feb 1500	3	DG	440	470	9	0	−22		
18 Feb 0246	18 Feb 1000	21 Feb 0000	2	41	520	700	8	2	−134	870	DG (16 Feb 0312)
10 March 0130	10 March 1700	12 March 1200	2	8	410	460	7	0	−78		
16 April 1125	16 April 1800	17 April 1900	1	18	400	450	20	2	−105	520	13 April 0330[g]
20 April 1600	21 April 0400	22 April 1600	1		500	620	8	1	−32		18 April 0830[j]
15 May 1600	15 May 1600	18 May 0000	2		390	400	5	0	−10		
2 June 2000	2 June 2300	3 June 2200	2		430	470	9	1	−6		
26 June 0325	26 June 0600	26 June 1900	3	8	350	350	15	1	−20	530	22 June 1854[g]
26 June 2016	27 June 1400	28 June 1400	3	36	680	880	8	0	−43	760	24 June 1331[g]
2 July 0059	2 July 2200	6 July 0600	2	11	450	650	5	0	−34		
6 July 1509	6 July 2100	8 July 0400	3	15	440	450	5	1	−8	620	3 July 1954
27 July 0000	27 July 1700	29 July 0600	3		390	430	6	0	−40	540	23 July 2130
30 July 1600	30 July 2000	31 July 0800	3		500	660	8	1	−60	710	28 July 0530[g,j]
31 July 1837	31 July 1900	2 Aug 0600	3	17	480	650	5	1	−37	497	28 July 0906[g]
2 Aug 1100	2 Aug 1400	3 Aug 1100	3		370	400	4	0	−21		
8 Aug 1841	8 Aug 1900	10 Aug 1700	2	0	360	420	9	2	−62		
11 Aug 2300	12 Aug 2000	14 Aug 0000	3		370	420	7	0	−24	615	9 Aug 0326
20 Aug 2300	20 Aug 2300	23 Aug 1600	2		450	570	8	1	−80	510	17 Aug 1331
22 Sept 1222	22 Sept 1900	24 Sept 1800	1	36	510	600	10	0	−164	700	20 Sep 0606[g]
21 Oct 0225	21 Oct 0800	22 Oct 0700	2	42	500	580	20	0	−231	480	18 Oct 0026[g]
11 Nov 1900	12 Nov 1000	13 Nov 1800	1		450	680	5	0	−100		DG
22 Nov 0000	22 Nov 0000	24 Nov 0300	3		450	490	9	0	−38		DG
12 Dec 1551	12 Dec 1900	13 Dec 1600	2	16	520	700	12	0	−92		DG
13 Dec 2300	14 Dec 0400	14 Dec 2000	2		440	480	12	0	−37		DG
26 Dec 2130[h]	27 Dec 1100	28 Dec 0400	2		430	450	8	1	−9		
					2000						
18 Jan 1500	19 Jan 0300	19 Jan 1500	2		270	330	7	0	−5		
22 Jan 0023	22 Jan 1700	23 Jan 0200	2		380	415	16	1	−91	530	18 Jan 1754[g]
11 Feb 0258	11 Feb 1600	11 Feb 2000	1	0	420	505	7	0	−25	630	8 Feb 0930[g]
11 Feb 2352	12 Feb 1200	13 Feb 0000	2	49	540	590	13	1	−169	900	10 Feb 0230[g]
14 Feb 0731	15 Feb 0000	16 Feb 0800	3	0	500	686	5	0	−88	730	12 Feb 0431[g]
20 Feb 2139	21 Feb 0500	22 Feb 1400	2	24	400	460	16	2	−20	570	17 Feb 2006[g]
1 March 0130	1 March 0300	2 March 0300	1		480	530	8	0	−49		
9 March 2300	10 March 0100	10 March 0600	2		390	400	6	1	0		
18 March 2200	19 March 0200	19 March 1200	1		380	390	9	0	−2		
29 March 1100	29 March 1900	31 March 2300	2		420	590	6	0	−58		
6 April 1639	7 April 0700	8 April 1800	2	74	550	620	5	1	−321	870	4 April 1632[g]
24 April 0400	24 April 0400	24 April 1400	2		490	520	13	0	−7		
27 April 1800	27 April 1800	28 April 0100	1		400	410	10	1	−15		
2 May 1045[h]	2 May 2000	5 May 1000	3		500	860	6	0	−38		29 April 0154[j]
6 May 1600	7 May 0000	8 May 1600	3		380	440	10	0	−4		
13 May 1700	13 May 1700	14 May 1800	2		500	600	8	0	0	603	10 May 2006
15 May 1900	15 May 1900	16 May 1200	3		430	450	8	0	−25		
16 May 2300	16 May 2300	17 May 0700	2		550	580	9	1	−88	500	13 May 1226
23 May 0700	23 May 1000	23 May 2100	2		570	610	12	1	0	650	20 May 1450
23 May 2300	24 May 1200	26 May 1600	2		550	690	5	1	−147	653	
4 June 1502	5 June 0000	6 June 2200	3	17	470	560	10	1	−35	403	31 May 0806
8 June 0910	8 June 1600	10 June 1700	3	59	550	790	10	0	−87	1100	6 June 1554[g]
11 June 0801	11 June 0700	11 June 1800	2	0	510	530	11	1	−41		
12 June 2208	13 June 1200	14 June 0600	2	0	440	550	7	0	−39		
18 June 0900	18 June 0900	18 June 1700	2		380	400	6	1	−9		
23 June 1303	24 June 0200	26 June 0800	2	37	500	590	8	0	−33		
26 June 1000	26 June 1000	27 June 0000	1		540	560	10	0	−74		
30 June 0700	30 June 0700	30 June 2300	2		380	400	6	0	−6		
1 July 0100	1 July 0600	3 July 0800	3		390	440	7	1	0		
10 July 0638	11 July 0200	11 July 1400	2	36	440	490	13	0	0	609	7 July 1026[g]
11 July 1123[h]	11 July 2200	13 July 0200	1		520	540	10	1	−24		
13 July 0942	13 July 1600	14 July 1500	2	31	620	700	7	0	−35	940	11 July 1327[g]
14 July 1532	14 July 1700	15 July 1400	2	29	780	800	9	1	−60		12 July 2030[j]
15 July 1437	15 July 1900	17 July 0800	2	120	850	980	20	2	−300	1600	14 July 1054[g]
19 July 1527	20 July 0100	21 July 0700	2	19	530	630	8	0	−95		17 July 0854[j]
23 July 1041	23 July 1500	25 July 0400	3	0	380	430	9	0	−66		DG
26 July 1857	27 July 0200	28 July 0200	2	0	360	400	6	1	−43	490	23 July 0530
28 July 0634	28 July 1200	30 July 1300	3	45	460	480	10	2	−74	580	25 July 0330[g]
10 Aug 0407[h]	10 Aug 1900	11 Aug 2100	1		430	490	12	1	−103		6 Aug 1830[j]
11 Aug 1845	12 Aug 0500	13 Aug 2200	1	21	580	670	16	2	−237	810	9 Aug 1630[g]
2 Sep 1300	2 Sep 2200	3 Sep 1300	1		430	450	8	0	−58		29 Aug 1830[j]

Table 1. (continued)

Disturbance Time,[b] UT	ICME Start, UT	ICME End, UT	Quality[c]	SC,[d] γ	V_{ICME}, km s^{-1}	V_{max}, km s^{-1}	B, nT	MC[e]	Dst, nT	V_T, km s^{-1}	LASCO CME[f]
8 Sep 1200	8 Sep 1800	10 Sep 1000	2		450	500	5	0	−44	530	5 Sep 0554
17 Sep 1657[h]	17 Sep 2300	21 Sep 0000	3		600	880	10	2	−172		15/16 Sep[i]
3 Oct 0054	3 Oct 1000	5 Oct 0300	1	0	400	430	14	2	−146		
5 Oct 0326	5 Oct 1300	7 Oct 1100	2	0	450	530	6	1	−192	580	2 Oct 2026[g]
12 Oct 2228	13 Oct 0800	14 Oct 1700	2	21	410	470	13	2	−110	580	9 Oct 2350[g]
20 Oct 1800	20 Oct 2200	21 Oct 0800	1		400	440	4	0	−2		
28 Oct 0954	28 Oct 2100	29 Oct 2200	2	35	380	420	14	2	−113	616	25 Oct 0826[g]
6 Nov 0948	6 Nov 2200	8 Nov 0300	3	18	510	610	20	2	−159		
10 Nov 0628	10 Nov 1000	11 Nov 0400	2	86	850	930	8	0	−104	1400	8 Nov 2306[g]
11 Nov 0400[h]	11 Nov 0800	12 Nov 0000	2		790	910	7	0	−43	1200	(9 Nov 1615)
26 Nov 1158	27 Nov 0800	28 Nov 0300	2	0	580	630	11	0	−72		24 Nov[i]
28 Nov 0530	28 Nov 1600	29 Nov 1900	2	24	530	590	10	1	−130	720	25/26 Nov[i]
					2001						
23 Jan 1048	24 Jan 0900	26 Jan 0800	1	30	400	550	5	1	−55	680	20 Jan 2130[g,i]
3 March 1121	4 March 0400	5 March 0200	2	0	440	520	8	0	−71	610	28 Feb 1450
19 March 1114	19 March 1700	21 March 2200	1	19	410	490	17	2	−165	520	16 March 0350
27 March 1747	28 March 0600	30 March 1900	3	26	520	650	4	0	−98	850	25 March 1706[g]
31 March 0052	31 March 0500	31 March 2200	3	105	640	710	39	1	−358	690	28 March 1250[g]
31 March 2200	1 April 0400	3 April 0300	2		640	820	5	0	0	700	29 March 1026[g]
4 April 1455	5 April 1100	7 April 0300	3	57	520	780	6	0	−38	1020	2 April 2206
8 April 1101	8 April 1900	10 April 1000	3	41	610	780	8	0	−51	1050	6 April 1930[g]
11 April 1343	11 April 2200	13 April 0700	2	0	640	740	14	2	−257	1220	10 April 0530[g]
13 April 0734	13 April 0900	14 April 1200	1	31	730	830	9	0	−66	970	11 April 1331[g]
18 April 0046	18 April 1200	20 April 1100	2	0	430	520	8	0	−100	580	
21 April 1601	21 April 2300	23 April 0800	1	19	350	390	11	2	−104		
28 April 0431[h]	28 April 1400	1 May 0200	2	58	540	730	8	2	−33	1080	26 April 1230[g]
7 May 0800	7 May 1900	8 May 0700	1		360	410	8	1	−24		
8 May 1101	9 May 1200	10 May 2200	2		430	560	8	1	−70		
11 May 1300	11 May 1300	12 May 0000	2		430	430	8	0	−40		
12 May 0920[h]	12 May 1700	13 May 1600	3		570	670	7	0	−46		10 May 0131[j]
15 May 1500	16 May 0900	17 May 0000	3		460	530	5	1	−20		
27 May 1459	28 May 0300	29 May 2100	1	0	460	600	8	2	−39		
30 May 0800	30 May 0800	31 May 0800	2		350	370	5	1	−2		
7 June 0852[h]	7 June 1800	8 June 0700	1		390	430	9	1	−4		
21 June 0300	21 June 0300	21 June 1000	3		570	600	5	1	−27		
26 June 1200	27 June 0300	28 June 1700	1		420	490	3	0	−18		
8 July 1200	9 July 0200	11 July 0400	2		400	460	4	1	−41	520	5 July 0354
13 July 1700	13 July 1700	14 July 0100	2		400	420	8	1	−8		
3 Aug 0716	3 Aug 1100	3 Aug 1400	3	0	420	440	10	0	−17		
15 Aug 0500	15 Aug 0500	16 Aug 1400	3		390	450	5	0	−16		
17 Aug 1103	17 Aug 2000	20 Aug 0000	2	29	490	600	10	0	−104	620	14 Aug 1601[g]
27 Aug 1952	28 Aug 2000	29 Aug 2000	3	20	470	580	4	0	−20	810	25 Aug 1650[g]
30 Aug 1411	30 Aug 2000	31 Aug 1000	2	0	420	500	6	1	−45		
1 Sep 1300	1 Sep 1300	2 Sept 1800	2		360	410	5	1	−17		
13 Sep 0200	13 Sep 1800	14 Sep 2200	2		410	440	10	1	−58		
23 Sep 1100	24 Sep 0000	25 Sep 0000	3		450	570	7	1	−77	700	20 Sep 1931
29 Sep 0940	30 Sep 0000	1 Oct 0000	2	0	520	700	12	1	−64		27 Sep 0454[j]
30 Sep 1924	1 Oct 0800	2 Oct 0000	2	0	490	550	9	0	−150	710	28 Sep 0854[g]
1 Oct 2200	2 Oct 1200	3 Oct 1600	2		510	530	13	1	−182	715	29 Sep 1154
11 Oct 1701	12 Oct 0200	12 Oct 1100	2	46	530	580	17	1	−74	770	9 Oct 1130[g]
21 Oct 1648	22 Oct 0000	25 Oct 1000	1	61	470	670	9	0	−166	860	19 Oct 1650[g]
26 Oct 2200	27 Oct 0000	28 Oct 0200	2		390	410	8	0	−28	417	23 Oct 1826
28 Oct 0319	29 Oct 2200	31 Oct 1300	2	48	360	510	4	0	−160	694	25 Oct 1526
31 Oct 1348	31 Oct 1800	2 Nov 1200	2	19	340	390	11	2	−97		
6 Nov 0152	6 Nov 2100	9 Nov 0600	2	110	570	750	6	0	−277	1240	4 Nov 1635[g]
19 Nov 1815	19 Nov 2200	20 Nov 1100	3	0	480	580	6	1	−32	680	17 Nov 0530[g]
24 Nov 0656	24 Nov 1400	26 Nov 1100	2	62	660	1000	12	2	−213	1300	22 Nov 2330[g]
27 Nov 0300	27 Nov 0300	27 Nov 1200	2		470	480	6	0	−27		
28 Dec 0000	28 Dec 0000	29 Dec 1200	2		360	370	8	0	0		
29 Dec 0538	30 Dec 0000	30 Dec 1400	2	78	400	460	17	1	−39	570	26 Dec 0530[j]
					2002						
15 Feb 1000	15 Feb 1000	15 Feb 1700	1		370	380	7	1	0	621	12 Feb 1506[g]
28 Feb 0451	28 Feb 1700	1 March 1000	2	46	390	410	13	1	−64		
18 March 1322	19 March 0500	20 March 1600	2	64	380	470	15	2	−41	667	15 March 2306
20 March 1328	21 March 1400	22 March 0600	3	15	440	580	8	0	−10		
23 March 1137	23 March 2100	25 March 2000	2	24	450	500	15	2	−101	625	20 March 1706[j]
12 April 0100	12 April 0100	13 April 1300	3		420	450	8	0	−20		
17 April 1107	17 April 2100	19 April 0900	2	54	480	610	12	1	−126		
19 April 0835	20 April 0000	21 April 1800	2	30	500	640	8	2	−152	863	17 April 0826[g]
20 May 0340	20 May 1500	21 May 2200	3	13	410	510	6	0	−33	420	16 May 0050[g]

Table 1. (continued)

Disturbance Time,[b] UT	ICME Start, UT	ICME End, UT	Quality[c]	SC,[d] γ	V_{ICME}, km s^{-1}	V_{max}, km s^{-1}	B, nT	MC[e]	Dst, nT	V_T, km s^{-1}	LASCO CME[f]
21 May 2203	22 May 1800	23 May 0500	3	17	420	440	9	0	−13		
23 May 1050	23 May 2000	25 May 1800	2	59	590	920	11	2	−108	1323	22 May 0326[g]
17 July 1603	18 July 1200	19 July 0900	3	0	460	520	6	0	−13	955	15 July 2030[g]
19 July 1450[h]	20 July 0400	22 July 0600	2	13	650	930	6	0	−33		
1 Aug 0510	1 Aug 0900	1 Aug 2300	2	26	450	460	12	2	−46		
1 Aug 2309	2 Aug 0400	4 Aug 0100	2	18	460	520	10	0	−85	505	29 July 1145
18 Aug 1846	19 Aug 1200	21 Aug 1400	2	44	460	580	8	1	−92	777	16 Aug 1230[g]
29 Aug 2100	29 Aug 2100	30 Aug 0600	2		400	420	8	1	−35		
7 Sep 1610[h]	8 Sep 0400	8 Sep 2000	2	DG	470	550	10	0	−164	882	5 Sep 1654[g]
8 Sep 2000	8 Sep 2200	10 Sep 2100	2	DG	440	520	9	0	−64		
19 Sep 0600	19 Sep 2000	20 Sep 2100	2	DG	490	750	5	0	−26	901	17 Sep 0754[g]
2 Oct 2210[h]	3 Oct 0100	4 Oct 1800	2	DG	430	520	11	2	−13		
17 Nov 0000	17 Nov 1000	18 Nov 1200	2	DG	380	500	8	2	−24		

[a]SC is geomagnetic storm sudden commencement; V_{ICME} is the mean solar wind speed in the ICME; V_{max} is the maximum solar wind speed in the postdisturbance region; B is the mean field strength; V_T is the transit speed; LASCO is the Large Angle and Spectrometric Coronagraph experiment; and DG is a LASCO data gap around the expected time of the associated CME.

[b]Time of the associated SC when present. Otherwise, the time of shock passage at ACE is given. If no shock or SC is reported, the estimated arrival time of the disturbance (which in some cases is also the ICME leading edge) is given to the nearest hour.

[c]Quality of the boundary times: 1, most accurate; 2, less accurate; 3, ill-defined.

[d]SC size is the mean horizontal component for midlatitude stations (from Solar-Geophysical Data).

[e]MC is magnetic cloud: 0, the field shows little evidence of rotation; 1, a more subjective assessment suggests evidence of a relatively organized field rotation within the ICME, but a magnetic cloud has not been reported; and 2, the ICME has been reported as a magnetic cloud which can be modeled by a force-free flux rope.

[f]Times in parentheses indicate associated solar events during an interval with no coronagraph coverage.

[g]CME had a 360° angular extent (i.e., halo CME).
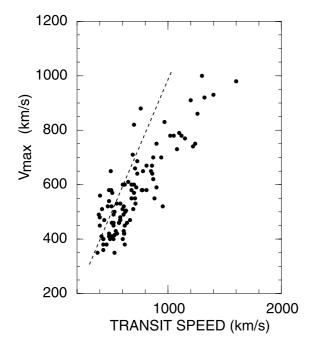
[h]Time of shock passage at ACE.

[i]ICMEs could result from multiple CMEs.

[j]CME association may be doubtful.

[1985, 1988] showed that this parameter is correlated with the shock compression ratio. No value or a value of 0 indicates that either no SC or a very weak SC was reported, respectively. This parameter is also used to validate associations. In some cases when an SC did not occur the disturbance time is the time of shock passage at the ACE spacecraft (ACE shocks were confirmed from the web site at http://www.bartol.udel.edu/~chuck/ace/ACElists/obs_list.html). The second and third columns give the estimated start and end times of the ICME, respectively, while the following column indicates the quality of the estimated boundary times (1, most accurate; 3, ill-defined; note that this parameter does not necessarily reflect the confidence of the ICME identification). The sixth and seventh columns give the mean speed of the ICME (V_{ICME}) and the maximum speed in the postdisturbance region (V_{max}), respectively, which may occur either in the "sheath" ahead of the ICME or in the ICME itself.

[18] The next column gives the mean field strength in the ICME. In the following column, "2" indicates whether the ICME has been reported as a magnetic cloud which can be modeled by a force-free flux rope (http://lepmfi.gsfc.nasa.gov/mfi/mag_cloud_pub1.html; for recent events since May 2002, not covered by this magnetic cloud list, we have assessed whether the ICME is likely to meet the criteria for a magnetic cloud). If a more subjective assessment suggests evidence of a relatively organized field rotation within the ICME but a magnetic cloud has not been reported, a "1" is indicated. A "0" indicates that the field shows little evidence of rotation. The third to last column gives the minimum value of the geomagnetic Dst index (stronger activity is denoted by an increasingly negative value). The disturbance transit speed to 1 AU is indicated in the next column for those events where the associated CME

observed by LASCO can be identified. The time of first observation of this CME in the LASCO C2 coronagraph is indicated in the last column; instances when the coronagraph signature encircled the Sun (i.e., had an angular extent of 360°, commonly called a "full halo" event) are noted. When making these associations, we have only considered CMEs with angular extents of at least 100°. For almost all of the energetic events the CME association is easily made because the shock driven by a fast ICME continuously accelerates energetic particles which directly link the passage of the shock at the Earth to the time of a specific CME at the Sun. For a variety of reasons, no CME is indicated for many of the ICMEs. One reason is that there are no LASCO observations around the time when the associated CME might have occurred, indicated by "DG" (data gap). In addition to the extended suspension of SOHO operations from June to October 1998, there are shorter interruptions to LASCO observations, often of several days duration, that are noted in the preliminary lists of LASCO CMEs. Where there is a LASCO data gap but the associated solar event is clearly identifiable from other data, the time is indicated in parentheses. There are other cases where LASCO observations are available but show no evidence of a large CME during the several days prior to arrival of the ICME at Earth, such as for the 19 June 1997 event discussed by *Richardson et al.* [1999]. It is likely that such ICMEs are associated with Earthward-directed CMEs that are not sufficiently dense to be detectable by LASCO. In other cases, one or more wide CMEs may be reported in this time range, but examination of the related solar activity as observed, for example, by the extreme ultraviolet imaging telescope suggests that these CMEs originated near the solar limbs or from the backside of the Sun and were unlikely to give rise to ICMEs at Earth based on the conclusions of our

Figure 1. Plot of the maximum solar wind speed (V_{max}) associated with an ICME versus the transit speed (V_T) of the disturbance from the Sun to the Earth. The lower limit to V_{max} for a particular transit speed permits some potential CME/ICME associations to be ruled out.

previous studies [e.g., *Richardson and Cane*, 1993; *Cane and Richardson*, 1995; *Cane et al.*, 1997, 2000]. At times of high activity there may be several wide CMEs with reasonable locations reported prior to an ICME so that it is difficult to relate the ICME to a specific CME. In these and other doubtful cases the time of the most likely associated CME is noted. The CME properties we have used here are from the work of S. Yashiro and G. Michalek (a catalog is available at http://cdaw.gsfc.nasa.gov/CME_list/). We have also referred back to the original LASCO observer reports since these are of value in indicating the general location of the related solar activity or in indicating whether the event was likely to be backsided and therefore of little interest for relating with in situ observations at Earth. Although we have focused on wide CMEs, we recognize, of course, that there are many more narrower CMEs observed by LASCO. However, our expectation is that these CMEs are unlikely to be related to ICMEs at Earth. Another point to note is that although we have attempted to isolate individual ICMEs, it is possible that some events are conglomerations of ICMEs from multiple solar ejections or, conversely, a series of events may be multiple encounters with a single ICME. However, we doubt that either of these situations occurs very often because, as discussed in section 3, the

relative change in ICME rate from solar minimum to maximum is similar to that in the CME rate. In Table 1, we indicate in the final column a small number of ICME periods that probably resulted from multiple CMEs [cf. *Burlaga et al.*, 2002].

[19] In making the CME/ICME associations we have found a good correlation between the maximum solar wind speed observed in situ at 1 AU in the sheath or ICME (V_{max}) and the transit speed (V_T) of the disturbance driven by the ICME to 1 AU for those events with a confident association (Figure 1). (A similar result has been previously obtained by *Cliver et al.* [1990].) In cases where the CME/ICME association is more uncertain this relationship can be used to indicate whether a particular association is at least plausible. For example, Figure 1 suggests that an ICME associated with $V_{max} = 500$ km s^{-1} is unlikely to be associated with a solar event <42 hours earlier that would require a transit speed above ~1000 km s^{-1}. Note that the transit speed is generally higher than V_{max} (the dashed line indicates $V_T = V_{max}$), implying that the disturbances decelerate en route to 1 AU. Furthermore, this deceleration is greater for higher transit speeds, consistent with the results of previous studies [e.g., *Woo et al.*, 1985]. For lower-speed events the transit and in situ speeds are more comparable and are similar to typical solar wind speeds (~400 km s^{-1}), consistent with their convection with the solar wind. Although it is possible to infer ICME acceleration rates and initial speeds as a function of V_{max} or transit speed from the results in Figure 1 by making a simple assumption such as a constant acceleration/deceleration rate in the solar wind [e.g., *Gopalswamy et al.*, 2001], such an assumption is questionable; we have not pursued this further.
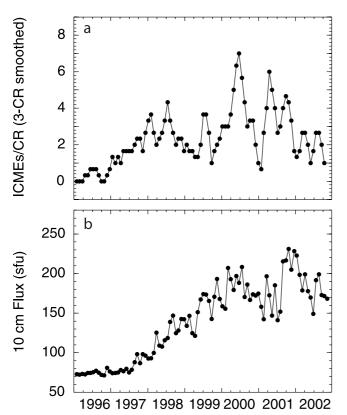
3. Occurrence Rates

[20] As might be expected, the yearly number of ICMEs increases with solar activity levels. During solar minimum conditions in 1996, only four ICMEs were identified, compared with 53 in 2000 and 47 in 2001 (see Table 2). Thus the ICME rate increased by about an order of magnitude from ~1 every 3 months at solar minimum to ~1 per week at solar maximum. These are average rates. At times of exceptionally high activity such as in May 1998, July 2000, or April 2001 the rate increases to several ICMEs per week (e.g., five ICMEs were observed between 11 and 18 July 2000). *Burlaga et al.* [1984] and *Cliver et al.* [1987] have discussed the possible consequences of such systems of transient flows passing the Earth during previous solar cycles. The decrease in the ICME rate in 1999 was noted in our previous study that only extended to this time [*Cane et al.*, 2000]. The rate increased again in the subsequent 2 years. A decline in the fraction of CME-related solar wind at

Table 2. Summary of Average ICME Properties

	1996[a]	1997	1998	1999	2000[b]	2001	2002	All
Number of events	4	22	38	28	53	47	22	214
ICME speed, km s^{-1}	360 ± 4	406 ± 11	428 ± 14	448 ± 13	490 ± 17	470 ± 14	452 ± 14	454 ± 6
ICME average B, nT	9.0 ± .7	12.9 ± 1.4	10.7 ± 0.6	9.4 ± 0.9	9.5 ± 0.5	8.8 ± 0.8	9.3 ± 0.6	9.9 ± 0.3
Magnetic cloud fraction, %	100	64	26	11	17	15	33	25

[a]Solar minimum.
[b]Solar maximum.

Figure 2. (a) Three-Carrington rotation (CR) running mean of the ICME rate (number of ICMEs per solar rotation) in 1996–2002. (b) CR average 10-cm flux of the Sun. Note that the 10-cm flux increases more uniformly than the ICME rate and in particular, does not show a significant decrease in 1999.

Earth in 1999 is also evident in Figure 3 of *Richardson et al.* [2002], together with a compensating increase in the contribution from corotating high-speed streams originating in low-latitude coronal holes, which were particularly prominent in 1999 [e.g., *Luhmann et al.*, 2002]. Thus the temporary decline in the ICME rate at Earth is associated with a restructuring of the near-ecliptic solar wind.

[21] Figure 2a shows the variation in the ICME rate during 1996–2002 in greater detail, specifically the number of ICMEs at Earth/Carrington rotation (CR) expressed as a three-rotation running mean. The main increase in the ICME rate, to ~2–3 CR^{-1}, commenced early in 1997 and extended through this year. Overall the rate has not varied greatly from this value during solar maximum with the exception of short intervals, typically of about three-rotation duration, when the ICME rate was enhanced due to major solar activity, as mentioned above. In addition, there is a decrease in the ICME rate to ~1–2 CR^{-1} during much of 1999 and a short duration decrease in late 2000 to early 2001. A typical rate of ~3 ICMEs CR^{-1} around solar maximum represents ~3% of the LASCO CME rate near maximum of ~4 d^{-1} (O. C. St Cyr, personal communication, 2002). It is also an order of magnitude higher than the ICME rate during 1996 at solar minimum (~0.3 ICMEs CR^{-1}), which is ~2% of the LASCO CME rate during this year (0.63 d^{-1} [*St. Cyr et al.*, 2000]).

[22] To compare the variations in the ICME rate with a measure of solar activity levels, Figure 2b shows the solar 10-cm flux recorded by the Dominion Radio Astrophysical Observatory. Note the two maxima during the first half of 2000 and the second half of 2001. (The smoothed sunspot number also shows two maxima, but the peak in April 2000 was slightly higher relative to the peak in November 2001 than in the 10-cm flux.) Assuming that our ICME rate is proportional to the CME rate, it can be seen that the rate does not follow the solar activity quite as closely as suggested by the work of *Webb and Howard* [1994]. The most significant difference is the reduction in 1999, which is not matched by a similar decrease in the 10-cm flux. The observations for 2002 show evidence for the expected reduction in the ICME rate as the solar cycle declines, the three-rotation mean rate never exceeding 3 ICMEs CR^{-1}.
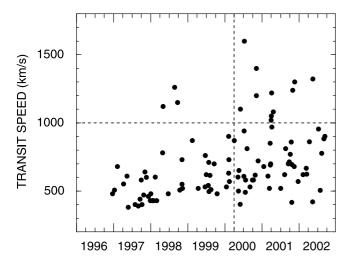
[23] An interesting feature of Figure 2a is the suggestion of periodicity in the intervals of enhanced ICME rate. A Lomb frequency analysis of the (unsmoothed) CME rate for 1996 to November 2002 indicates a dominant, statistically significant component with a period of 164.7 days. This period is particularly interesting since it is close to the "154-day" periodicity identified in various solar phenomena during previous solar cycles [see *Cane et al.*, 1998b, and references therein]. The apparent periodicity in the ICME rate suggests that the fundamental periodicity at the Sun identified in previous solar cycles is present in the current cycle, as also noted in energetic particle intensities at 1 and 5 AU in 1998–1999 by *Dalla et al.* [2001].

4. Average Properties of ICMEs

[24] Table 2 lists the average properties of ICMEs and their variation as a function of year. Another clear solar cycle variation is evident in the fraction of the ICMEs that are magnetic clouds. This decreased from 100% (though with poor statistics) in 1996 to ~16% in 2000–2001 and appears to be recovering in 2002 as activity declines. Data from previous solar cycles support such a solar cycle variation (I. G. Richardson and H. V. Cane, The fraction of interplanetary coronal mass ejections that are magnetic clouds, submitted to *Geophysical Research Letters*, 2003).

[25] Average speeds of individual ICMEs varied from 270 to 850 km s^{-1} with a mean value of 454 ± 6 km s^{-1}. The mean speed shows a ~100 km s^{-1} increase from solar minimum to maximum. This increase is also evident in Figure 4b of *Richardson et al.* [2002], which, however, suggests that this trend may be specific to cycle 23 since the previous two solar cycles show instead a temporary minimum in mean ICME speeds near solar maximum. The transit speed of the associated disturbance is also ordered by the phase of the solar cycle in that there were only three shocks with transit speeds >1000 km s^{-1} during the ~4.5 years before solar (smoothed sunspot) maximum (April 2000) versus 11 thus far in the first ~2.5 years after maximum (Figure 3). It is such fast shocks that are responsible for large >10 MeV particle events [*Cane et al.*, 1988].

[26] Average magnetic field strengths in individual ICMEs varied from 3 to 39 nT with a mean value of 9.9 ± 0.3 nT. There is a slight decrease in average fields from minimum to maximum. This is primarily related to the fact that the fraction of magnetic clouds decreased toward

Figure 3. Transit speeds of the shocks/disturbances associated with those ICMEs that can be related to CMEs observed by the LASCO coronagraphs (or with a solar event if LASCO observations are not available). Note that more events with speeds >1000 km s^{-1} (indicated by the dashed horizontal line) occur after solar maximum in early 2000 (indicted by the dashed vertical line) than before this time.

maximum. The average ICME size in the radial direction (the product of the duration and average speed) was 0.33 ± 0.01 AU. For those events (typically the more energetic) that we could associate with a solar event (usually an H α flare) the longitudes were predominantly within ±50° of central meridian, as shown by the "source" longitude distribution in Figure 4. This result suggests that ICMEs associated with the more energetic solar events have angular extents of up to ~100°, as previously inferred by Richardson and Cane [1993]. An interesting feature of the distribution is the occasional presence at Earth of ICMEs from far western regions but not from far eastern regions. A similar asymmetry in the source longitude distribution was found by Cane [1988] for helium abundance enhancements (which, as noted above, may be indicative of ICMEs) in cycle 21, suggesting that this is a general feature. A possible explanation for the asymmetry in Figure 4 [see also Wang et al., 2002, Figure 3a] is that some CMEs preferentially occur to the east of the active region where the associated flare occurred (i.e., the flare is not necessarily centered beneath the CME). This has a natural explanation in terms of differential rotation, which causes shearing and eastward motion of erupted magnetic flux in both hemispheres of the Sun.

5. Solar-Terrestrial Relations

[27] There has been much emphasis in recent years on the relationship between CMEs of large angular extent observed by LASCO that appear to be moving toward or away from the Earth approximately along the Sun-Earth line (i.e., halo CMEs) and the effects of the associated ICMEs when they arrive at Earth ~2 days later [e.g., St. Cyr et al., 2000; Webb et al., 2000]. However, as we have noted previously [Cane et al., 2000], there is certainly not a simple one-to-one relationship between large CMEs (with

associated frontside solar activity) and ICMEs observed subsequently at Earth. We concluded that in 1996–1999, about a third of the ICMEs detected at Earth were not preceded by a >140° CME evident in LASCO observations. In Table 1, it is evident that we cannot associate many of the ICMEs with large CMEs. In some cases this is because there were no LASCO observations around the probable time that the related CME might have occurred (indicated by "DG"). We conclude that a significant fraction, about a half, of the ICMEs detected at Earth do not have a probable association with a large CME observed by LASCO. Cane et al. [2000] also found that only about half of the frontside >140°-width CMEs observed by LASCO subsequently encountered the Earth. For the additional years of the current study (2000 and 2001) we find that even if only those events which surround the Sun are considered (i.e., full halo events with angular extents of 360°), the fraction is only ~39%. This contrasts with the situation in 1997, when all the frontside full halo CMEs resulted in the detection of ICMEs near Earth [see also Zhao and Webb, 2003]. We suggest that when the corona is close to its solar minimum configuration, 360° coronagraph events result from CMEs directed at (or away from) the Earth as is commonly assumed. However, later in the solar cycle (approaching and during solar maximum) the corona is much more complex, and coronagraph observations may include more contributions from other phenomena such as streamer deflections [e.g., Sheeley et al., 2000] that give rise to features surrounding the Sun even when the associated CME is not directed at the Earth.

[28] In Figure 5, we compare the disturbance transit speeds to 1 AU with the speeds of the associated CMEs.
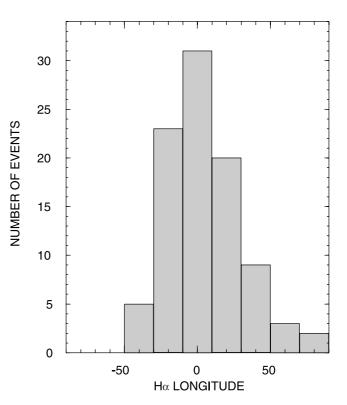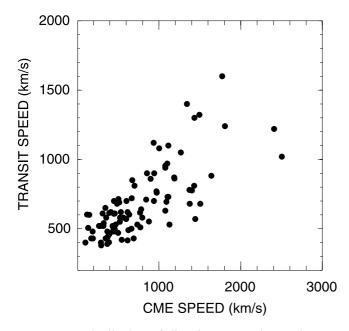

Figure 4. Distribution of the longitudes of the solar chromospheric events associated with ICMEs at the Earth.

Figure 5. Distribution of disturbance transit speeds as a function of the sky plane speeds of the associated CMEs.

Although the CME speeds are projected against the plane of the sky and do not represent the true Earthward-directed speeds of the CMEs, there is nonetheless some degree of correlation, as we have noted previously [*Cane et al.*, 2000]. The upper envelope of the distribution is given approximately by $V_T = 400 + 0.8V_{CME}$ (this defines the minimum transit time for a given CME speed), while the lower envelope is approximately $V_T = 0.37V_{CME}$. The observed transit speeds do not fall below $\sim$400 km s^{-1}. Given the considerable scatter among the data points, however, it seems unrealistic to expect that the transit speed for a given CME speed can be predicted precisely. Note that we consider here the disturbance speed because this corresponds to the earliest time when a CME may produce a disturbance at Earth. *Gopalswamy et al.* [2000, 2001] have developed an empirical model to predict ICME arrival times based on LASCO CME speeds. For CME speeds below $\sim$700 km s^{-1} an ICME transit time to 1 AU of $\sim$4.3 days (corresponding to a transit speed $\sim$400 km s^{-1}) that is independent of CME speed is predicted [see *Gopalswamy et al.*, 2001, Figure 6]. The observations in Figure 5 suggest that the disturbance transit speeds range over $\sim$400–800 km s^{-1} for similar CME speeds. Thus the *Gopalswamy et al.* [2001] $\sim$4.3-day prediction should not be assumed to give (and generally overestimates) the time taken for relatively slow CMEs to produce effects at Earth.

[29] In Table 1, we have recorded the size of the geomagnetic disturbance caused by each ICME and/or its associated "sheath" as measured by the minimum value of the *Dst* index. Figure 6 shows the distribution of the values for minimum *Dst* as a function of time, with magnetic cloud events represented by solid circles. The solar cycle dependence of the relative occurrence of magnetic clouds noted above is readily apparent, being more dominant in 1996–1997 than in later years. Although some large storms are caused by ICMEs that are not magnetic clouds, relative to their overall numbers magnetic clouds are

responsible for a disproportionate fraction of the largest storms, most likely because by definition they include stronger than average fields as well as large rotations in field direction which may give rise to intervals of southward magnetic fields that drive geomagnetic activity. Another feature of Figure 6 is the general absence of strong storms in 1999. In addition to there being fewer ICMEs in this year, their magnetic field strengths were also weaker on average (see Table 2). This helps to account for the slightly lower fraction (50%) of the full halo CMEs which impacted the Earth that produced strong storms ($Dst < -50$) in this year compared with 80% in other years. Finally, we note the tendency for the strongest storms to occur following solar maximum.
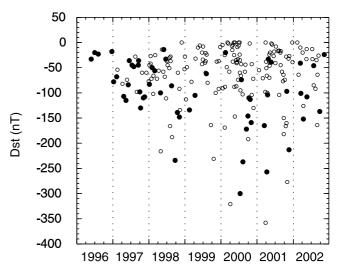
6. Summary

[30] We have prepared a comprehensive list of ICMEs recorded near Earth during the period 1996 through November 2002. We find the following:

[31] 1. The rate of ICMEs increased by about an order of magnitude from solar minimum to solar maximum but only approximately followed solar activity variations as indicated by the 10-cm flux (or sunspot number). The ICME rate is $\sim$3% of the CME rate observed by LASCO.

[32] 2. The fraction of ICMEs that have well-organized, flux rope-like magnetic field structures (magnetic clouds) decreased from $\sim$100% at solar minimum to $\sim$15% around solar maximum and may be recovering as activity declines. Relative to their numbers, magnetic clouds are responsible for a disproportionate fraction of major geomagnetic storms.

[33] 3. The fastest disturbances and strongest geomagnetic storms related to ICMEs tend to occur after solar maximum.

[34] 4. The vast majority of energetic ICMEs originated from solar events located within $\sim$50° of central meridian.

Figure 6. Distribution of minimum geomagnetic *Dst* values during the passage of the ICMEs or the related sheath regions as a function of time. Solid circles represent events that were magnetic clouds. Although these generally produce stronger geomagnetic effects, not all strong ICME-related storms result from magnetic clouds. Note that a larger fraction of ICMEs are magnetic clouds in 1996 and 1997.

However, there is an asymmetry in the source region distribution, suggesting that sometimes CMEs form or propagate to the east of the associated active region.

[35]   5. The ICME rate shows a ~165-day periodicity that may be consistent with the "~154-day" periodicity previously reported in various solar data sets.

References

Bame, S. J., J. R. Asbridge, W. C. Feldman, E. E. Fenimore, and J. T. Gosling, Solar wind heavy ions from flare-heated coronal plasma, *Sol. Phys.*, *62*, 179, 1979.

Barnden, L. R., The large-scale magnetic configuration associated with Forbush decreases, *Cosmic Ray Conf. Pap. Int. Conf. Cosmic Rays 13th*, *2*, 1277, 1972.

Borrini, G., J. T. Gosling, S. J. Bame, and W. C. Feldman, Helium abundance enhancements in the solar wind, *J. Geophys. Res.*, *87*, 7370, 1982.

Brueckner, G. E., et al., The large angle spectroscopic coronagraph (LASCO), *Sol. Phys.*, *162*, 357, 1995.

Burlaga, L. F., and K. W. Ogilvie, Solar wind temperature and speed, *J. Geophys. Res.*, *78*, 2028, 1973.

Burlaga, L. F., E. Sittler, F. Mariani, and R. Schwenn, Magnetic loop behind an interplanetary shock: Voyager, Helios, and Imp 8 observations, *J. Geophys. Res.*, *86*, 6673, 1981.

Burlaga, L. F., F. B. McDonald, N. F. Ness, R. Schwenn, A. J. Lazarus, and F. Mariani, Interplanetary flow systems associated with cosmic ray modulation in 1977–1980, *J. Geophys. Res.*, *89*, 6579, 1984.

Burlaga, L. F., S. P. Plunkett, and O. C. St. Cyr, Successive CMEs and complex ejecta, *J. Geophys. Res.*, *107*(A10), 1266, doi:10.1029/2001JA000255, 2002.

Cane, H. V., The evolution of interplanetary shocks, *J. Geophys. Res.*, *90*, 191, 1985.

Cane, H. V., The large-scale structure of flare-associated interplanetary shocks, *J. Geophys. Res.*, *93*, 1, 1988.

Cane, H. V., Coronal mass ejections and Forbush decreases, *Space Sci. Rev.*, *93*, 55, 2000.

Cane, H. V., and I. G. Richardson, Cosmic ray decreases and solar wind disturbances during late October 1989, *J. Geophys. Res.*, *100*, 1755, 1995.

Cane, H. V., D. V. Reames, and T. T. von Rosenvinge, The role of interplanetary shocks in the longitude distribution of solar energetic particles, *J. Geophys. Res.*, *93*, 9555, 1988.

Cane, H. V., I. G. Richardson, T. T. von Rosenvinge, and G. Wibberenz, Cosmic ray decreases and shock structure: A multispacecraft study, *J. Geophys. Res.*, *99*, 21,429, 1994.

Cane, H. V., I. G. Richardson, and T. T. von Rosenvinge, Cosmic ray decreases: 1964–1994, *J. Geophys. Res.*, *101*, 21,561, 1996.

Cane, H. V., I. G. Richardson, and G. Wibberenz, Helios 1 and 2 observations of particle decreases, ejecta, and magnetic clouds, *J. Geophys. Res.*, *102*, 7075, 1997.

Cane, H. V., I. G. Richardson, and O. C. St. Cyr, The interplanetary events of January–May, 1997, as inferred from energetic particle data, and their relationship with solar events, *Geophys. Res. Lett.*, *25*, 2517, 1998a.

Cane, H. V., I. G. Richardson, and T. T. von Rosenvinge, Interplanetary magnetic field periodicity of 153 days, *Geophys. Res. Lett.*, *25*, 4437, 1998b.

Cane, H. V., I. G. Richardson, and O. C. St. Cyr, Coronal mass ejections, interplanetary ejecta, and geomagnetic storms, *Geophys. Res. Lett.*, *27*, 3591, 2000.

Cliver, E. W., J. D. Mihalov, N. R. Sheeley Jr., R. A. Howard, M. J. Koomen, and R. Schwenn, Solar activity and heliosphere-wide cosmic ray modulation in mid-1982, *J. Geophys. Res.*, *92*, 8487, 1987.

Cliver, E. W., J. Feynman, and H. B. Garrett, An estimate of the maximum speed of the solar wind, 1938–1989, *J. Geophys. Res.*, *95*, 17,103, 1990.

Crooker, N. U., J. T. Gosling, E. J. Smith, and C. T. Russell, A bubblelike coronal mass ejection flux rope in the solar wind, in *Physics of Magnetic Flux Ropes*, *Geophys. Monogr. Ser.*, vol. *58*, edited by C. T. Russell, E. R. Priest, and L. C. Lee, p. 365, AGU, Washington, D.C., 1990.

Dalla, S., A. Balogh, B. Heber, and C. Lopate, Further indications of a ~140 day recurrence in energetic particle fluxes at 1 and 5 AU from the Sun, *J. Geophys. Res.*, *106*, 5721, 2001.

Dere, K. P., G. E. Brueckner, R. A. Howard, D. J. Michels, and J. P. Delaboudiniere, LASCO and EIT observations of helical structure in coronal mass ejections, *Astrophys. J.*, *516*, 465, 1999.

Fenimore, E. E., Solar wind flows associated with hot heavy ions, *Astrophys. J.*, *235*, 245, 1980.

Gopalswamy, N., A. Lara, R. P. Lepping, M. L. Kaiser, D. Berdichevsky, and O. C. St. Cyr, Interplanetary acceleration of coronal mass ejections, *Geophys. Res. Lett.*, *27*, 145, 2000.

Gopalswamy, N., A. Lara, S. Yashiro, M. L. Kaiser, and R. A. Howard, Predicting the 1-AU arrival times of coronal mass ejections, *J. Geophys. Res.*, *106*, 29,207, 2001.

Gosling, J. T., Coronal mass ejections and magnetic flux ropes in interplanetary space, in *Physics of Magnetic Flux Ropes*, *Geophys. Monogr. Ser.*, vol. *58*, edited by C. T. Russell, E. R. Priest, and L. C. Lee, p. 343, AGU, Washington, D. C., 1990.

Gosling, J. T., V. Pizzo, and S. J. Bame, Anomalously low proton temperatures in the solar wind following interplanetary shock waves: Evidence for magnetic bottles?, *J. Geophys. Res.*, *78*, 2001, 1973.

Gosling, J. T., D. N. Baker, S. J. Bame, W. C. Feldman, R. D. Zwickl, and E. J. Smith, Bidirectional solar wind electron heat flux events, *J. Geophys. Res.*, *92*, 8519, 1987.

Gosling, J. T., J. Birn, and M. Hesse, Three-dimensional magnetic reconnection and the magnetic topology of coronal mass ejection events, *Geophys. Res. Lett.*, *22*, 869, 1995.

Gosling, J. T., R. M. Skoug, and W. C. Feldman, Solar wind electron halo depletions at 90° pitch angle, *Geophys. Res. Lett.*, *28*, 4155, 2001.

Hirshberg, J., S. J. Bame, and D. E. Robbins, Solar flares and solar helium enrichments: July 1965–July 1967, *Sol. Phys.*, *23*, 467, 1972.

Ipavich, F. M., A. B. Galvin, G. Gloeckler, D. Hovestadt, S. J. Bame, B. Klecker, M. Scholer, L. A. Fisk, and C. Y. Fan, Solar wind Fe and CNO measurements in high-speed flows, *J. Geophys. Res.*, *91*, 4133, 1986.

Klein, L. W., and L. F. Burlaga, Interplanetary magnetic clouds at 1 AU, *J. Geophys. Res.*, *87*, 613, 1982.

Lepping, R. P., J. A. Jones, and L. F. Burlaga, Magnetic field structure of interplanetary magnetic clouds at 1 AU, *J. Geophys. Res.*, *95*, 11,957, 1990.

Lepri, S. T., T. H. Zurbuchen, L. A. Fisk, I. G. Richardson, H. V. Cane, and G. Gloeckler, Iron charge distribution as an identifier of interplanetary coronal mass ejections, *J. Geophys. Res.*, *106*, 29,231, 2001.

Lopez, R. E., Solar cycle invariance in solar wind proton temperature relationships, *J. Geophys. Res.*, *92*, 11,189, 1987.

Luhmann, J. G., Y. Li, C. N. Arge, P. R. Gazis, and R. Ulrich, Solar cycle changes in coronal holes and space weather cycles, *J. Geophys. Res.*, *107*(A8), 1154, 10.1029/2001JA007550, 2002.

Marsden, R. G., T. R. Sanderson, C. Tranquille, K.-P. Wenzel, and E. J. Smith, ISEE 3 observations of low-energy proton bidirectional events and their relation to isolated interplanetary magnetic structures, *J. Geophys. Res.*, *92*, 11,009, 1987.

McGuire, R. E., T. T. von Rosenvinge, and F. B. McDonald, The composition of solar energetic particles, *Astrophys. J.*, *301*, 938, 1986.

Mitchell, D. G., E. C. Roelof, and S. J. Bame, Solar wind iron abundance variations at speeds >600 km s^{-1}, 1972–1976, *J. Geophys. Res.*, *88*, 9059, 1983.

Montgomery, M. D., J. R. Asbridge, S. J. Bame, and W. C. Feldman, Solar wind electron temperature depressions following some interplanetary shock waves: Evidence for magnetic merging?, *J. Geophys. Res.*, *79*, 3103, 1974.

Morrison, P., Solar origin of cosmic ray time variations, *Phys. Rev.*, *101*, 1397, 1956.

Neugebauer, M., and R. Goldstein, Particle and field signatures of coronal mass ejections in the solar wind, in *Coronal Mass Ejections*, *Geophys. Monogr. Ser.*, vol. *99*, edited by N. Crooker, J. A. Joselyn, and J. Feynman, p. 245, AGU, Washington, D. C., 1997.

Neugebauer, M., J. T. Steinberg, R. L. Tokar, B. L. Barraclough, E. E. Dors, R. C. Wiens, D. E. Gingerich, D. Luckey, and D. B. Whiteaker, Genesis on-board determination of the solar wind flow regime, *Space Sci. Rev.*, in press, 2003.

Osherovich, V., and L. F. Burlaga, Magnetic clouds, in *Coronal Mass Ejections*, *Geophys. Monogr. Ser.*, vol. *99*, edited by N. Crooker, J. A. Joselyn, and J. Feynman, p. 157, AGU, Washington, D. C., 1997.

Palmer, I. D., F. R. Allum, and S. Singer, Bidirectional anisotropies in solar cosmic ray events: Evidence for magnetic bottles, *J. Geophys. Res.*, *83*, 75, 1978.

Richardson, I. G., and H. V. Cane, Signatures of shock drivers in the solar wind and their dependence on the solar source location, *J. Geophys. Res.*, *98*, 15,295, 1993.

Richardson, I. G., and H. V. Cane, Regions of abnormally low proton temperature in the solar wind (1965–1991) and their association with ejecta, *J. Geophys. Res.*, *100*, 23,397, 1995.

Richardson, I. G., and H. V. Cane, Particle flows observed in ejecta during solar event onsets and their implication for the magnetic field topology, *J. Geophys. Res.*, *101*, 27,521, 1996.

Richardson, I. G., and D. V. Reames, Bidirectional ∼1 MeV ion intervals in 1973–1991 observed by the Goddard Space Flight Center instruments on IMP 8 and ISEE 3/ICE, *Astrophys. J. Suppl. Ser.*, *85*, 411, 1993.

Richardson, I. G., H. V. Cane, and T. T. von Rosenvinge, Prompt arrival of solar energetic particles from far eastern events: The role of large-scale interplanetary magnetic field structure, *J. Geophys. Res.*, *96*, 7853, 1991.

Richardson, I. G., H. V. Cane, and O. C. St. Cyr, Relationships between coronal and interplanetary structures inferred from energetic particle observations, in *Solar Wind Nine*, edited by S. R. Habbal et al., *AIP Conf. Proc.*, *471*, 677, 1999.

Richardson, I. G., V. M. Dvornikov, V. E. Sdobnov, and H. V. Cane, Bidirectional particle flows at cosmic ray and lower (∼1 MeV) energies and their association with interplanetary coronal mass ejections/ejecta, *J. Geophys. Res.*, *105*, 12,597, 2000.

Richardson, I. G., E. W. Cliver, and H. V. Cane, Sources of geomagnetic storms for solar minimum and maximum conditions during 1972–2000, *Geophys. Res. Lett.*, *28*, 2569, 2001a.

Richardson, I. G., V. M. Dvornikov, V .E. Sdobnov, and H. V. Cane, Bidirectional cosmic ray and ∼1 MeV ion flows, and their association with ejecta, *Conf. Pap. Int. Cosmic Ray Conf. 27th*, *9*, 3498, 2001b.

Richardson, I. G., H. V. Cane, and E. W. Cliver, Sources of geomagnetic activity during nearly three solar cycles (1972–2000), *J. Geophys. Res.*, *107*(A8), 1187, doi:10.1029/2001JA000504, 2002.

Sheeley, N. R., Jr., R. A. Howard, M. J. Koomen, D. J. Michels, R. Schwenn, K. H. Mühlhäuser, and H. Rosenbauer, Coronal mass ejections and interplanetary shocks, *J. Geophys. Res.*, *90*, 163, 1985.

Sheeley, N., Jr., W. N. Hakala, and Y.-M. Wang, Detection of coronal mass ejection associated shock waves in the outer corona, *J. Geophys. Res.*, *105*, 5081, 2000.

St. Cyr, O. C., et al., Properties of coronal mass ejections: SOHO LASCO observations from January 1996 to June 1998, *J. Geophys. Res.*, *105*, 18,169, 2000.

Wang, Y. M., P. Z. Ye, S. Wang, G. P. Zhou, and J. X. Wang, A statistical study on the geoeffectiveness of Earth-directed coronal mass ejections from March 1997 to December 2000, *J. Geophys. Res.*, *107*(A11), 1340, doi:10.1029/2002JA009244, 2002.

Webb, D. F., and R. A. Howard, The solar cycle variation of coronal mass ejections and the solar wind mass flux, *J. Geophys. Res.*, *99*, 4201, 1994.

Webb, D. F., E. W. Cliver, N. U. Crooker, and O. C. St. Cyr, Relationship of halo coronal mass ejections, magnetic clouds, and magnetic storms, *J. Geophys. Res.*, *105*, 7491, 2000.

Woo, R., J. W. Armstrong, N. R. Sheeley Jr., R. A. Howard, M. J. Koomen, D. J. Michels, and R. Schwenn, Doppler scintillation observations of interplanetary shocks within 0.3 AU, *J. Geophys. Res.*, *90*, 154, 1985.

Zhao, X. P., and D. F. Webb, Source regions and storm effectiveness of frontside full halo coronal mass ejections, *J. Geophys. Res*, doi:10.1029/2002JA009606, in press, 2003.

Zwickl, R. D., J. R. Asbridge, S. J. Bame, W. C. Feldman, and J. T. Gosling, He^+ and other unusual ions in the solar wind: A systematic search covering 1972–1980, *J. Geophys. Res.*, *87*, 7379, 1982.

Zwickl, R. D., J. R. Asbridge, S. J. Bame, W. C. Feldman, J. T. Gosling, and E. J. Smith, Plasma properties of driver gas following interplanetary shocks observed by ISEE-3, in *Solar Wind Five*, edited by M. Neugebauer, *NASA Conf. Publ.*, *2280*, 711, 1983.

———————

H. V. Cane and I. G. Richardson, Laboratory for High Energy Astrophysics, Code 661, NASA Goddard Space Flight Center, Greenbelt, MD 20771, USA. (hilary.cane@utas.edu.au; richardson@lheavx.gsfc.nasa.gov)